

# Distribution of IR and Submillimeter Line Emitting Galaxies in Cosmological Simulations

NATUKI HAYATSU,<sup>1</sup> NAOKI YOSHIDA,<sup>2</sup> AND YUICHI MATSUDA<sup>3,4</sup>

<sup>1</sup>*Department of Physics, University of Tokyo, Japan*

<sup>2</sup>*Department of Physics, and Kavli IPMU, University of Tokyo, Japan*

<sup>3</sup>*National Astronomical Observatory of Japan, Mitaka, Tokyo*

<sup>4</sup>*The Graduate University for Advanced Studies (SOKENDAI)*

## ABSTRACT

We present a forecast for detection of high-redshift star-forming galaxies using *SPICA*-SAFARI and ALMA Band 10–11. We use the outputs of large cosmological simulations of galaxy formation to calculate the fluxes of infrared and far-infrared emission lines ([O III]88.3  $\mu\text{m}$ , [O III] 51.8  $\mu\text{m}$ , [N III]57.2  $\mu\text{m}$  and [C II]158  $\mu\text{m}$ ). To this end, we assume empirical relations between the line fluxes and the star formation rate or far-infrared luminosities. We consider a large survey programme with a  $2' \times 2'$  field-of-view and the limiting flux densities of  $> 21$  and  $> 32 \mu\text{Jy}$  ( $5\sigma$ ). Our models predicts that there are  $604 \pm 59$  galaxies to be detected by such a survey. The number of [C II] emitters with  $L_{[\text{C II}]} < 10^9 L_\odot$  is expected to be  $543 \pm 52$ .

## 1. INTRODUCTION

The chemical evolution and star-formation activities of high-redshift galaxies will be studied by high-resolution mm/submm/IR observations by *SPICA* and ALMA. Infrared fine structure lines such as [O III]51.8  $\mu\text{m}$ , [N III]57.21  $\mu\text{m}$  and [O III]88.3  $\mu\text{m}$  can be used as metallicity diagnostics (Nagao et al. 2011), whereas [C II]158  $\mu\text{m}$  line is thought to be an ideal tracer of star-formation activity. The particular emission line can also constrain the metallicity of a high redshift galaxy in combination with [N II] 205  $\mu\text{m}$  (Nagao et al. 2012).

In order to address the feasibility of observations of high-redshift galaxies, we use the results of a large cosmological hydrodynamics simulation of galaxy formation. Throughout this paper we adopt the  $\Lambda$ -CDM cosmology with the matter density  $\Omega_M = 0.27$ , the cosmological constant  $\Omega_\Lambda = 0.73$ , the Hubble constant  $h = 0.7$  in units of  $H_0 = 100 \text{ km s}^{-1} \text{ Mpc}^{-1}$ , the baryon density  $\Omega_B s = 0.046$ .

## 2. METHOD

We use one of the cosmological simulations in Shimizu et al. (2012). Briefly, the simulation employs  $2 \times 640^3$  particles in a comoving volume of  $100 h^{-1} \text{ Mpc}$  on a side. The mass of a dark matter particle is  $2.41 \times 10^8 h^{-1} M_\odot$  and that of a gas particle is  $4.95 \times 10^7 h^{-1} M_\odot$ . They implement relevant physical processes such as star formation, supernovae and galactic wind feedback and chemical enrichment. We calculate the SEDs of individual galaxies using the population synthesis code PEGASE2. Then, wavelength-dependent dust absorption is calculated such that the resulting UV luminosity function at high redshifts matches to the result of recent observations. In order to calculate FIR luminosity  $L_{\text{FIR}}$ , we assume that the UV photons absorbed by thermal dust grains are re-emitted in FIR. Namely, we set  $L_{\text{FIR}}$  to be equal to the total energy of UV photons absorbed:

$$L_{\text{FIR}} = \int [L^{\text{int}}(\nu) - L^{\text{real}}(\nu)] d\nu \quad (1)$$

where  $L^{\text{int}}(\nu)$  is the intrinsic luminosity (per frequency) of the galaxy and  $L^{\text{real}}$  is the luminosity after absorption. The above integration is evaluated from UV to optical wavelengths. The model reproduces UV luminosity function at  $z = 2.5$ . Furthermore, the source number counts of SMGs for observed frame of 850  $\mu\text{m}$  and 1.1 mm are consistent with observation (Shimizu et al. 2012).

In order to calculate the [C II], [N III] and [O III] luminosities, we adopt empirical relations calibrated by mostly observations of local star-forming galaxies. We calculate [C II] luminosity  $L_{[\text{C II}]}$  using the following three empirical laws:

$$L_{[\text{C II}]} / L_{\text{FIR}} = (L_{\text{FIR}} / L_\odot)^{-0.157} \times 10^{-1.12}, \quad (2)$$

$$\text{SFR} / (M_\odot / \text{yr}) = (L_{[\text{C II}]} / L_\odot)^{0.987} \times 10^{-7.0}, \quad (3)$$

$$\text{SFR} / (M_\odot / \text{yr}) = (L_{[\text{C II}]} / L_\odot) \times 10^{-7.08}. \quad (4)$$

The first is derived from Swinbank et al. (2012) (hereafter  $L_{[\text{C II}]}^{\text{Sw}}$ ). The last two equations are derived from De Looze et al. (2012) and Sargsyan et al. (2012) (hereafter  $L_{[\text{C II}]}^{\text{De}}$ ,  $L_{[\text{C II}]}^{\text{Sa}}$ ). We compare the resulting luminosity functions based on the three relations in Figure 1. Clearly, there is little model dependence.

HAYATSU, YOSHIDA, AND MATSUDA

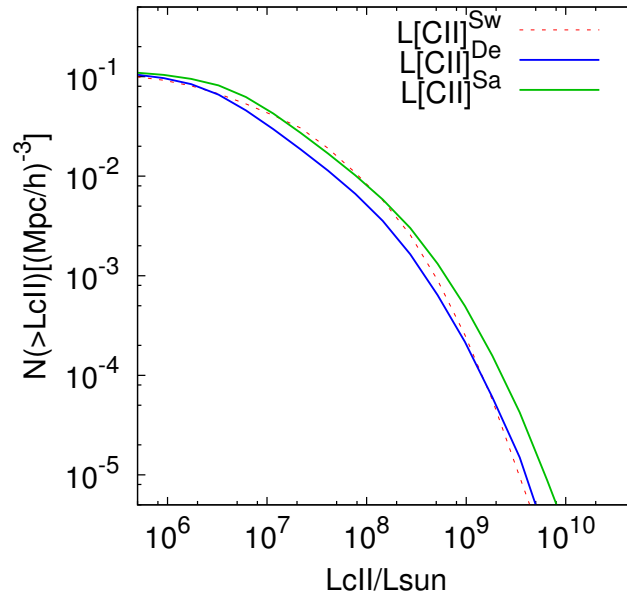


**Figure 1.** [C II] luminosity function at  $0.6 < z < 3.05$ .

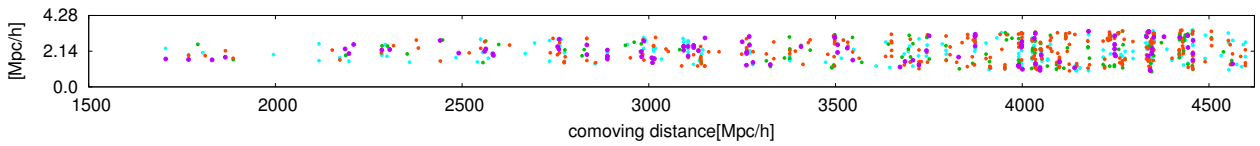


**Figure 2.** SMGs with submm line fluxes greater than  $20 \mu\text{Jy}$  at  $z < 3.05$ . The field of view is  $2' \times 2'$ . The colour indicates the flux density  $F$  of [O III]51.8 :  $20 \mu\text{Jy} < F < 50 \mu\text{Jy}$  (cyan),  $50 \mu\text{Jy} < F < 100 \mu\text{Jy}$  (green),  $100 \mu\text{Jy} < F < 1 \text{mJy}$  (orange),  $1 \text{mJy} < F$  (magenta).

We also use simple relations between  $L_{\text{FIR}}$  and other fine structure lines (Nagao et al. 2011):

$$(L_{[\text{O III}]88.33}/L_{\text{FIR}}) = 1.8 \times 10^{-3}, \quad (5)$$

$$(L_{[\text{O III}]51.80}/L_{\text{FIR}}) = 1.8 \times 10^{-3}, \quad (6)$$

$$(L_{[\text{N III}]57.21}/L_{\text{FIR}}) = 6.0 \times 10^{-4}. \quad (7)$$

### 3. LINE DETECTION BY SPICA-SAFARI AND ALMA

The *SPICA-SAFARI* with band-pass  $34\text{--}210 \mu\text{m}$  can detect [O III]51.80  $\mu\text{m}$  emission from galaxies at  $z < 3.05$ . If we also detect [O III]88.33 and [N III]57.21, we can utilize the metallicity diagnostics of SMGs by measuring  $([\text{O III}]51.80 + 88.33) / [\text{N III}]57.21$  (Nagao et al. 2011). In order to detect these two lines, we consider another observation of ALMA Band 10 and 11, or CCAT. Let us consider combination of *SPICA-SAFARI* and ALMA. With the high sensitivity of *SPICA*, faint ( $< 10^9 L_{\odot}$ ) [C II] emitters can be detected.

The field of views of *SPICA-SAFARI* is  $2' \times 2'$ , and the limiting source flux densities within 1 hour are estimated to be 21, 32  $\mu\text{Jy}$  ( $5\sigma$ ) for the 2 channels, respectively. We adopt this condition and repeat 10 times to calculate scatter. The flux density  $F$  is given by

$$F = 0.96 \times 10^3 \frac{(L/L_{\odot})(1+z)}{d_L^2 \Delta\nu \nu_{\text{rest}}} \quad [\text{Jy}], \quad (8)$$

where  $L$  is luminosity in erg/s,  $d_L$  is luminosity distance in Mpc,  $\nu_{\text{rest}}$  is rest frequency of the line in GHz, and  $z$  is redshift. We assume line width of  $\Delta\nu = 120 \text{ km/s}$  for simplicity.

### 4. RESULT

We plot the spatial distribution of our simulated SMGs on the past light cone of an observer in Figure 2.

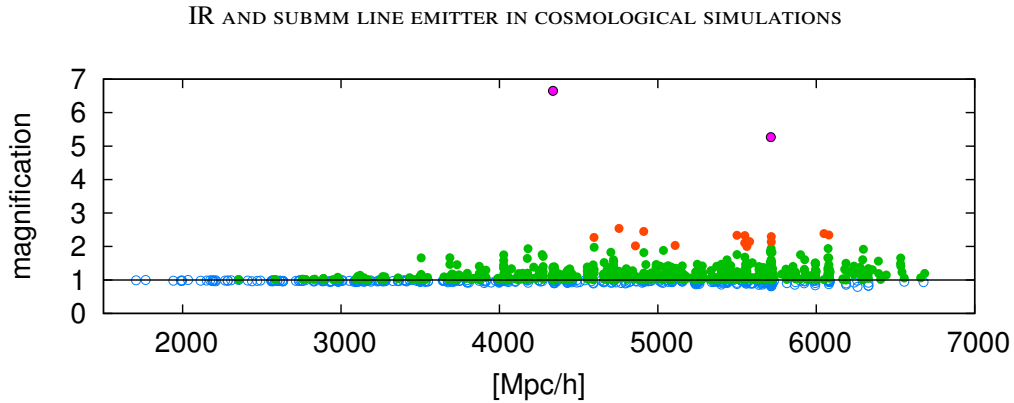


**Figure 3.** Gravitational lensing magnification of our simulated galaxies in a field of view of  $1' \times 1'$  at  $z < 10$ .

For our proposed survey, the number of SMGs to be detected is  $604 \pm 59$  (Max: 727, min: 534). The corresponding value of [C II] emitters whose luminosity  $L_{[\text{C II}]_{\text{SW}}} < 10^9 L_{\odot}$  is  $543 \pm 52$  (Max: 655, min: 482). We also consider effect of the gravitational lensing (Takahashi et al. 2011). Several sources can be strongly lensed, but lensing does not affect considerably to the expected number counts (Figure 3).

Our calculations adopting empirical laws provide an educated estimate of the number counts. However, we cannot examine the metallicity diagnostics in this way, because the calculated line ratios do not depend on the metallicity. We plan to develop a physical model of line emissions that utilize the output of cosmological simulations.

The authors acknowledge support from NAOJ Visiting Fellow Program.

## REFERENCES

- De Looze, I., Baes, M., Bendo, G. J., Cortese, L., & Fritz, J. 2012, MNRAS, 416, 2712  
 Nagao, T., Maiolino, R., De Breuck, C., et al. 2012, A&A, 542, L34  
 Nagao, T., Maiolino, R., Marconi, A., & Matsuhara, H. 2011, A&A, 526, A149  
 Sargsyan, L., Leibouteiller, V., Weedman, D., et al. 2012, ApJ, 755, 171  
 Shimizu, I., Yoshida, N., & Okamoto, T. 2012, MNRAS, 427, 2866  
 Swinbank, A. M., Karim, A., Smail, I., et al. 2012, MNRAS, 427, 1066  
 Takahashi, R., Oguri, M., Sato, M., & Hamana, T. 2011, ApJ, 742, 15